Effect of Microstructure on Detonation Performance of the Insensitive High Explosive PBX 9502

Stephen J. Voelkel, Eric K. Anderson, Mark Short, Carlos Chiquete, Scott I. Jackson
Los Alamos National Laboratory
Los Alamos, New Mexico, USA

1 Introduction

Insensitive high explosives (IHEs) are an important class of explosives for applications that require a significant level of safety involving non-shock insults, but also require detonation performance properties approaching those of conventional high explosives. Examples of IHEs include PBX 9502, LX-17 and EDC35 [1]. These polymer-bonded formulations use 1,3,5-triamino-2,4,6-trinitrobenzene (TATB) as the high explosive (HE) crystal which are bound with KEL F-800 or FK-800, a co-polymer of chlorotrifluoro-ethylene and vinylidene-fluoride. PBX 9502 consists of 95 wt.% TATB with 5 wt.% KEL-F 800 (FK 800), and is formed from molding powder pressed to a target density of 1.890 ± 0.005 g/cm^3. The theoretical maximum density of PBX 9502 is 1.941 g/cm^3. It has a nominal Chapman-Jouguet (CJ) detonation speed of 7.8 mm/μs and a CJ pressure in the range of 28 GPa.

PBX 9502 has been in use as an IHE since the late 1970s, and subsequently many different batches of PBX 9502 molding powder have been manufactured. Each batch is assigned a designation known as a material lot. PBX 9502 lots that are pressed directly from raw molding powder are called virgin lots. However, since the TATB manufacturing process is expensive, a second type of lot was introduced, known as recycled lots [2]. Such lots use 50 wt.% of TATB recovered from machining scraps of pressed molding powder. The pressing process is believed to significantly fracture and damage the TATB crystals, and sieve analysis on TATB recovered from molding powder shows that recycled lots generally have a higher percentage of finer particles compared to virgin lots [2, 3]. This raises the potential of a performance difference in terms of detonation timing and metal push characteristics due to the microstructure differences between virgin and recycled lots. This question is investigated in the current article.

Gustavsen et al. [2] studied PBX 9502 shock initiation characteristics for ambient virgin and recycled PBX 9502 lots by comparing the run-to-detonation distance for various shock-loading states. The authors were not able to identify any significant lot-to-lot differences within the standard deviation of experimental error. Hill et al. [3] examined detonation performance timing variations between two virgin and two recycled PBX 9502 lots by comparing diameter effect and detonation shock shape differences. However, their analysis was limited by one of the virgin lots having data only at one diameter, and one of the recycled lots having no front shape data. Hill and Aslam [4] subsequently fitted a detonation shock dynamics model to the lots examined in [3]. Importantly though, detonation performance variations cannot be evaluated with timing alone, which is largely controlled by the detonation driving zone structure

Correspondence to: svoelkel@lanl.gov

(the region between the detonation shock and sonic flow locus), which itself depends significantly on the rate of reaction [5]. Detonation performance evaluations must also include both the comparison of the overall energy release (heat of detonation) and an analysis of the capability of the explosive products to push a surrounding confiner, such as metal, through an isentropic pressure release process.

In the following, we describe several new detonation performance characterization rate-stick and cylinder tests on a virgin, newly formulated PBX 9502 lot (designation BAE18D755–001) and a recycled legacy PBX 9502 lot (HOL88B891–007). This data is then combined with legacy experimental data for a virgin lot (HOL88H891–008) and a recycled lot (HOL85F000E–136) (both from [3]). Hereafter, we refer to lot designation BAE18D755–001 as 001, HOL88B891–007 as 007, HOL88H891–008 as 008 and HOL85F000E–136 as 136. Detonation shock dynamics model calibrations are conducted on each of the four lots, using both diameter effect and detonation front shape data in each case, to provide the basis for an assessment of the detonation timing characteristics of recycled vs. virgin PBX 9502 lots. Detonation product Jones-Wilkins-Lee equations of state (EOSs) are obtained from cylinder tests for lots 001, 007 and 008 to provide an assessment of the metal push capabilities of these lots. We find that the metal push capabilities, characterized by the evolution in heat of detonation with volume, are very similar between the virgin and recycled lots, but that detonations in virgin lots, on average, run slower than those in recycled lots. We surmise that this is due to a slower rate of reaction in virgin lots associated with the larger TATB particle sizes, and the resulting effect this has on the amount of energy release that occurs within the detonation driving zone (DDZ) [5]. The magnitude of the timing difference is shown to be geometry dependent.

2 Detonation Timing for Lot Dependent PBX 9502

In order to compare diameter effect and detonation front-shape variations between virgin and recycled PBX 9502 lots, we conducted four new unconfined, varying-diameter, rate-stick geometry experimental tests on the virgin lot 001 and three on the recycled lot 007. These measure the 2D axial steady detonation speed via ionization wire time-of-arrival diagnostics, and detonation front-shape (more specifically the arrival times of the detonation along a fixed radial line) using streak camera imaging, for each charge diameter. Specific testing methodologies are described in [6]. All tests were conducted at ambient conditions, nominally 25°C. The densities (ρ_0) of the 001 lot tests were $\rho_0 \approx 1.895$ g/cm^3, while those for the 007 tests were $\rho_0 \approx 1.893$ g/cm^3. The results of these tests are shown in Figs. 1 and 2, and will be discussed in the context of virgin to recycled lot variability below. We have not attempted to account for density variations within the pressing tolerance range (1.890$\pm$0.005 g/cm^3) for a given lot due to a lack of statistically relevant data.

A Detonation Shock Dynamics (DSD) propagation law for the PBX 9502 001 and 007 lots was calibrated from the experimental diameter effect and radial line breakout times. The DSD surface motion model assumes that the normal speed of the surface (D_n) at any point on the surface is a function of its local curvature (κ). The functional form of the D_n-κ relationship is given by

$$D_n(\kappa) = D_{CJ}\left[1 - B\kappa\left(\frac{1 + C_2\kappa}{1 + C_4\kappa}\right)\right], \tag{1}$$

where D_{CJ} is the CJ detonation velocity and B, C_2 and C_4 are function parameters to be calibrated, along with the angle that the DSD surface makes with the edge of the HE. A merit function minimization procedure is used to fit the DSD model parameters to the breakout time record and axial speed of the detonation for each charge size. The minimization procedure is described in [7], and conducted within HEDCAPE (High Explosive Detonation Calibration and Parameterization Environment). Additionally, corresponding DSD model calibrations based on previously published diameter effect and breakout time

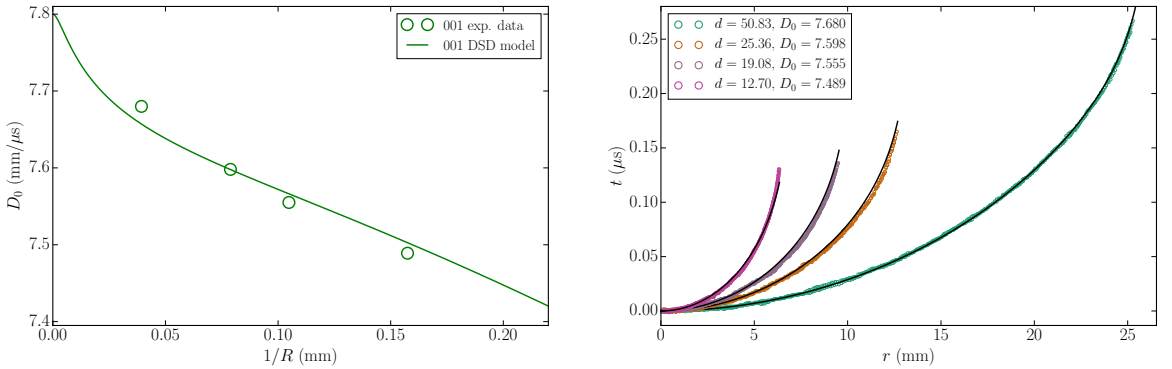

Figure 1: DSD model calibration of lot 001 showing comparisons of (left) the fitted diameter effect and (right) the fitted breakout time records with experimental data. Here, d is the rate-stick diameter, R the radius, r the radial coordinate, and D_0 is the steady detonation speed in the axial direction.

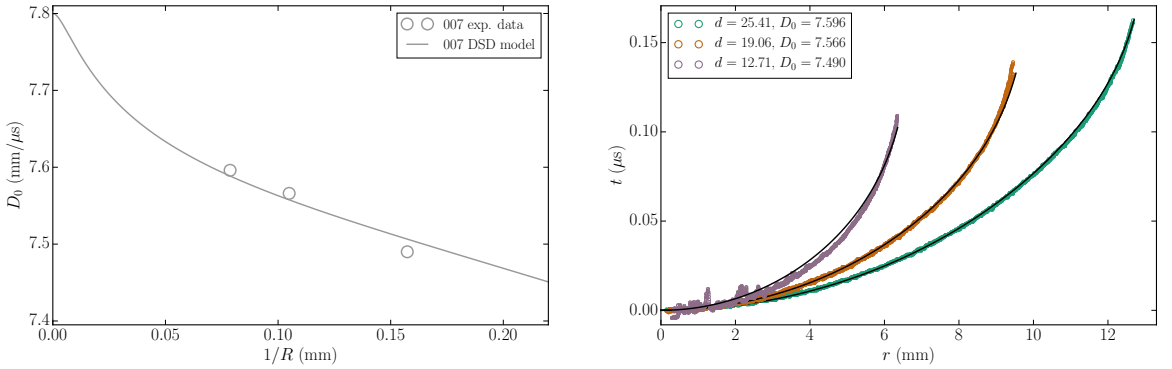

Figure 2: As for Fig. 1, but for lot 007.

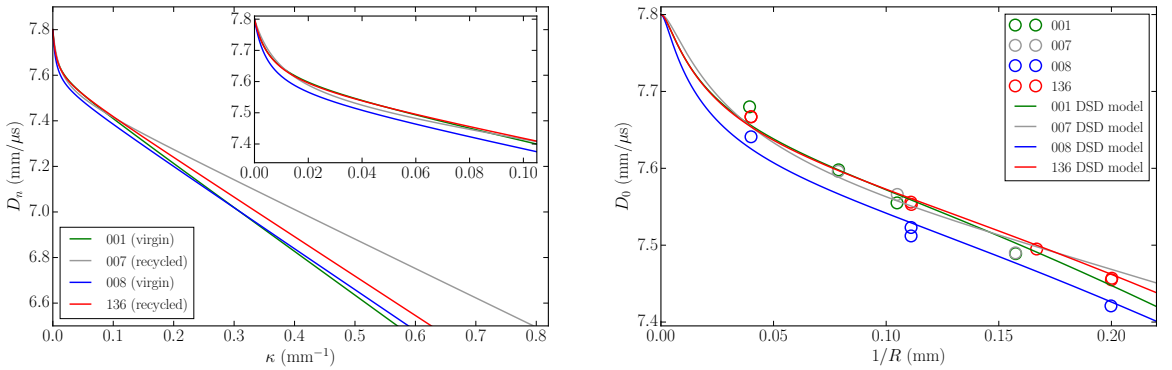

Figure 3: (Left) D_n vs. κ variation for each lot from the calibrated DSD model. (Right) Diameter effect variation for each lot showing comparisons of experimental data with the fitted DSD model.

data for the virgin lot 008 (includes three tests with $\rho_0 = 1.886$ g/cm^3 and one at $\rho_0 = 1.890$ g/cm^3) and recycled lot 136 (includes four tests with $\rho_0 \approx 1.892$ g/cm^3 and three with $\rho_0 = 1.895$ g/cm^3) [3] were conducted using the same merit function to prevent any biasing in the calibration.

Figure 3 (left) shows the DSD model-based $D_n - \kappa$ variation between the four PBX 9502 lots. For any curvature $\kappa < 0.01$, lot 007 has a marginally higher D_n than 001 and 136. Between $0.01 < \kappa < 0.09$, the 007 D_n field drops slightly below that of 001 and 136, which have similar variations. For curvatures in the range $\kappa > 0.09$, lot 007 has significantly higher D_n values than lots 001 and lot 136, with D_n also now larger for the recycled lot 136 than the virgin lot 001. Lot 008 has a D_n field that is lower than the other lots for $\kappa < 0.25$, while for $\kappa > 0.25$, 008 is close to the $D_n - \kappa$ variation for lot 001. However, limited information can be gained on lot timing differences from the $D_n - \kappa$ variation alone.

Specifically, the detonation speed and breakout time record are determined by an integrated effect of the $D_n - \kappa$ variation, which is strongly influenced by geometry and the different κ regions accessed in each geometry. That said, lot 008 would generally appear to have slower detonation speeds relative to the other three lots. The diameter effect points for the four lots and their fitted DSD model curves are shown in Fig. 3 (right). The three lots 001, 007 and 136 have similar axial detonation speeds for any given R, while 008 is lower. Plotting the κ and D_n variations vs. radial coordinate shows that for given R, the κ variations across the charge are very similar except at the edge. It is the lower values of D_n for given κ that causes 008 to run slower. To a great extent this is influenced by the energy release that occurs within the DDZ and therefore it is likely that 008 has slower kinetics relative to the other lots.

Detonation propagation in a 2D circular arc configuration highlights the effects of different regions of curvature being accessed. A PBX9502 lot 136 arc test was described in Short et al. [5] and consisted of an ≈ 65.0 mm inner radius and ≈ 90.0 mm outer radius arc. Detonation propagation in a circular arc is strongly influenced by the larger curvature variations seen in a layer next to the inner surface. A DSD calculation for the 65.0 x 90.0 mm arc geometry for each lot predicts that on the inner surface, the linear speed would be 7.146 mm/μs for lot 008, 7.166 mm/μs for lot 001, 7.182 mm/μs for lot 136 and 7.199 mm/μs and for lot 007. Recycled lot 007 runs significantly faster.

3 Detonation Push for Lot Dependent PBX 9502

In addition to the timing data, we have conducted three new cylinder expansion test geometry (CYLEX) experiments for lots 001, 007 and 008 (unfortunately, no legacy lot 136 material was available to the authors at the time of testing). Each was nominally a 1-inch-scale-test, consisting of a 25.4 mm diameter cylindrical HE charge, surrounded by a cylindrical oxygen-free, high-conductivity copper (Cu) tube with a wall thickness of 2.54 mm. As the detonation propagates axially, the detonation products expand, pushing the copper tube into a lateral motion. The radial velocity component of the Cu wall motion is measured by Photon-Doppler-Velocimetry (PDV) diagnostics as described in [6]. The CYLEX tests allow us to examine any variation in push provided by detonation products between the different lots, and also to calibrate a JWL EOS for the products. The HE density for the 001 test was $\rho_0 = 1.896$ g/cm^3, for 007 $\rho_0 = 1.895$ g/cm^3, and for 008 $\rho_0 = 1.891$ g/cm^3. The evolution in Cu wall motion in the radial direction for the three PBX 9502 lot tests is shown in Fig. 4.

The JWL EOS is of Mie-Gruneisen form based on a reference curve describing the pressure (p_s) variation with volume (v) along the principal isentrope, i.e. that passing through the CJ point. The pressure along the principal isentrope takes the form

$$p_s = A \exp\left[-R_1 v/v_0\right] + B \exp\left[-R_2 v/v_0\right] + C v^{-1-\omega}, \tag{2}$$

where C is a label for the principal isentrope, v_0 ($= 1/\rho_0$) is the initial specific volume of the HE, and A, R_1, B, R_2 and ω are the JWL EOS parameters. The associated internal energy variation along the principal isentrope is given by

$$e_s = \int_v^\infty p_s \, dv = \frac{A v_0}{R_1} \exp\left[-R_1 v/v_0\right] + \frac{B v_0}{R_2} \exp\left[-R_2 v/v_0\right] + \frac{C}{\omega} v^{-\omega}, \tag{3}$$

with the reference point set so that $e_s \to 0$ as $v \to \infty$. For states off the principal isentrope, the Mie-Gruneisen EOS form is $p = p_s + \omega(e - e_s)/v$, for pressure p and internal energy e. The area under the isentrope from $v = v_{CJ}$ to $v = \infty$ minus the area under the Rayleigh line defines the overall heat of detonation e_0, such that $e_s(v_{CJ}) - p_{CJ}(v_0 - v_{CJ})/2 = e_0$. The evolution in the heat of detonation with volume going from $v = v_{CJ}$ to $v = \infty$ is given by $e_0 - e_s(v) = e_s(v_{CJ}) - e_s(v) - p_{CJ}(v_0 - v_{CJ})/2$.

For each lot, we calibrate the JWL EOS model parameters A, B, R_1, R_2 and ω using a merit function minimization approach, whereby each CYLEX experiment is simulated in a Lagrangrian hydrocode

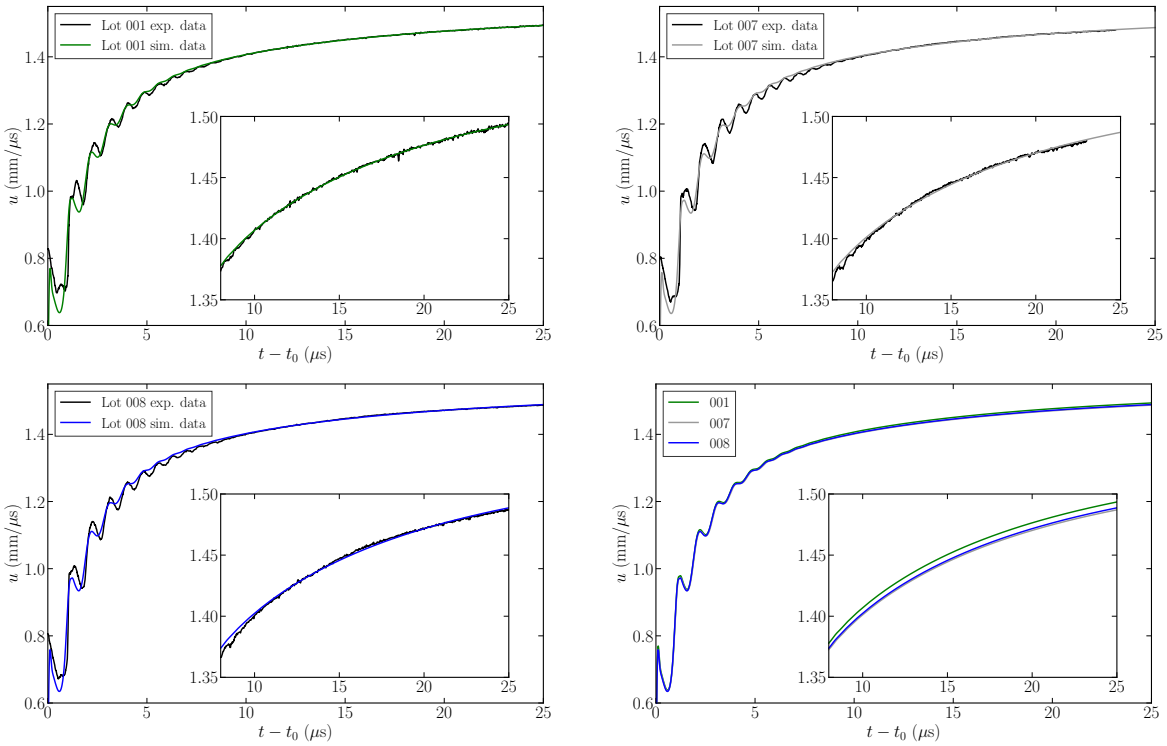

Figure 4: Velocity (u) of the radial component of the Cu wall motion with time (t) for lots 001, 007 and 008 relative to the time of wall motion start t_0. The experimental traces are constructed from an average of PDV probes aligned angularly around the tube at two different axial positions. Also shown is a comparison with the simulated wall motions for the final calibrated JWL EOS model for each lot. The lower right plot shows a comparison of the model wall motion calculations between the lots.

using a DSD-based programmed burn (PB) method. The simulated and experimentally measured wall expansion profiles (Fig. 4) are compared and A, B, R_1, R_2 and ω iterated on. The DSD model calibrated to each specific lot above is used for the timing, while the HE energy release in the PB simulation is calculated through a velocity-adjusted JWL method [8]. This strategy accounts for the influence of detonation front curvature on the evolution of the detonation products. For given A, B, R_1, R_2 and ω, the heat of detonation e_0 is set so that $D_{CJ} = 7.8$ mm/μs, corresponding to the DSD model for each lot.

The principal isentrope variation for lots 001, 007 and 008 is shown in Fig. 5. The corresponding variation in the heat of detonation with volume is shown in Fig. 6. Significantly, there is no major variation between the three lots. Lot 001 has a slight larger value of e_0 than lots 007 and 136, but the difference is not significant within the standard deviation of experimental error. Based on the cylinder tests and JWL product EOS calibration, we thus conclude that the total energy content between the virgin and recycled lots are very similar, and that metal push capabilities, characterized by the evolution in heat of detonation with volume, are therefore similar. However, as noted, detonations in virgin lots, on average, run slower than those in recycled lots. We have surmised that this is due to a slower rate of reaction in virgin lots associated with the larger TATB particle sizes, and the resulting effect this has on the amount of energy release that occurs within the DDZ. Thus, changes in microstructure between different PBX 9502 lots seemingly affect the rate of reaction, but not the overall energy content.

References

[1] C.A. Handley, B.D. Lambourn, N.J. Whitworth, H.R. James, and W.J. Belfield. Understanding the shock and detonation response of high explosives at the continuum and meso scales. *Appl. Phys.*

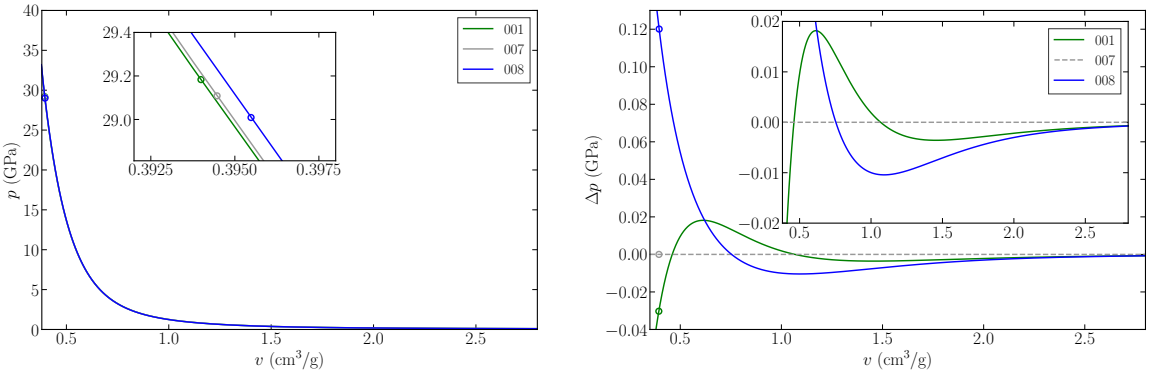

Figure 5: (Left) Comparison of the principal isentropes for lots 001, 007 and 008. (Right) Lot 001 and 008 pressure difference (Δp) along their principal isentropes relative to lot 007. The circles indicated the CJ state for each lot.

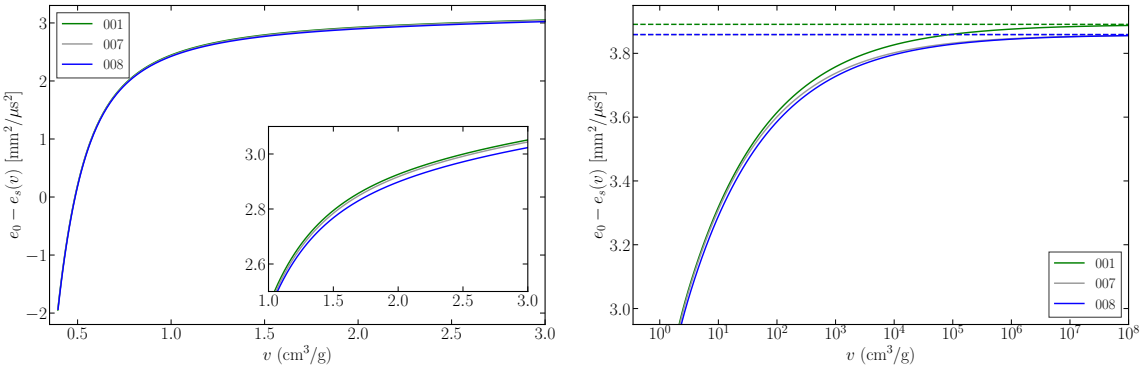

Figure 6: Heat of Detonation variation with volume v for each lot.

Rev., 5:011303, 2018.

[2] R.L. Gustavsen, S.A. Sheffield, and R.R. Alcon. Measurements of shock initiation in the tri-amino-tri-nitro-benzene based explosive PBX 9502: Wave forms from embedded gauges and comparison of four different material lots. *J. Appl. Phys.*, 99(11):114907, 2006.

[3] L. G. Hill, J. B. Bdzil, W. C. Davis, and R. R. Critchfield. PBX 9502 front curvature ratestick data: repeatability and the effects of temperature and material variation. In *13th Intl. Deton. Symp.*, number ONR 351-07-01 in Office of Naval Research, pages 331–341, 2006.

[4] L.G. Hill and T.D. Aslam. Detonation shock dynamics calibration for PBX 9502 with temperature, density, and material lot variations. In *14th Intl. Deton. Symp.*, number ONR-351-10-185 in Office of Naval Research, pages 779–788, 2010.

[5] M. Short, C. Chiquete, J.B Bdzil, and J.J. Quirk. Detonation diffraction in a circular arc geometry of the insensitive high explosive PBX 9502. *Combust. Flame*, 196:129–143, 2018.

[6] E.K. Anderson, C. Chiquete, S.I. Jackson, R.I. Chicas, and M. Short. The comparative effect of HMX content on the detonation performance characterization of PBX 9012 and PBX 9501 high explosives. *Combust. Flame*, 230:111415, 2021.

[7] C. Chiquete, M. Short, E. K. Anderson, and S. I. Jackson. Detonation shock dynamics modeling and calibration of the HMX-based conventional high explosive PBX 9501 with application to the two-dimensional circular arc geometry. *Combust. Flame*, 222:213–232, 2020.

[8] C. Chiquete and S.I. Jackson. Detonation performance of the CL-20-based explosive LX-19. *Proc. Combust. Instit.*, 38:3661–3669, 2021.